Micromechanical measurements on P-protein aggregates (forisomes) from plants

S. Schwan, M. Menzel, M. Fritzsche, A. Heilmann, U. Spohn

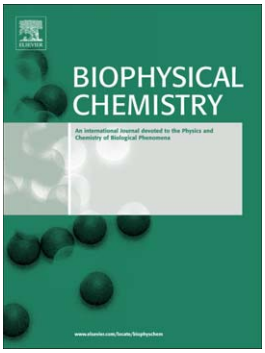

Micromechanical measurements on P-protein aggregates (forisomes) from *Vicia faba* plants

S. Schwan, M. Menzel, M. Fritzsche, A. Heilmann, U. Spohn

PII: S0301-4622(08)00227-5
DOI: doi: 10.1016/j.bpc.2008.10.008
Reference: BIOCHE 5179

To appear in: *Biophysical Chemistry*

Received date: 10 September 2008
Revised date: 23 October 2008
Accepted date: 23 October 2008

Please cite this article as: S. Schwan, M. Menzel, M. Fritzsche, A. Heilmann, U. Spohn, Micromechanical measurements on P-protein aggregates (forisomes) from *Vicia faba* plants, *Biophysical Chemistry* (2008), doi: 10.1016/j.bpc.2008.10.008

Micromechanical measurements on P-protein aggregates (forisomes) from *Vicia faba* plants

S. Schwan*, M. Menzel, M. Fritzsche, A. Heilmann, U. Spohn

Fraunhofer Institute of Mechanics of the Materials, Heideallee 19, D-06120 Halle, Germany

*Corresponding author: Tel. 0049 345 55 89 282, Fax 0049 345 55 89 101, sw@iwmh.fhg.de

Key words: P- protein aggregates, chemo-mechanical activity, influence of metal ions and pH, force measurement

Abstract

Forisomes are chemomechanically active P-protein aggregates found in the phloem of legumes. They can convert chemical energy into mechanical work when induced by divalent metal ions or changes in pH, which control the folding state of individual forisome proteins. We investigated the changing geometric parameters of individual forisomes and the strength and dynamics of the forces generated during this process. Three different divalent ions were tested (Ca^{2+}, Sr^{2+} and Ba^{2+}) and were shown to induce similar changes to the normalized length and diameter. In the concentration range from 0.1 to 4 M, K^{+} and Cl^{-} ions had no influence on the contraction behaviour of the forisomes induced by 10 mM Ca^{2+}. In the absence of dissolved oxygen, these changes were independent of the radius of the metal ion, water uptake and the strength of binding between the selected metal ions and those protein molecules responsible for forisome conformational transformation. In the absence of any load, bound Ca^{2+}, Sr^{2+} and Ba^{2+} ions showed apparent and averaged dissociation constants of 14, 62 and 1070 μM, respectively. Various forisomes generated bending on a quartz glass fibre with a diameter of 9 μm. The fibre bending was measured microscopically also by correlation between the digital patterns of a predefined window of observation before and after bending. Similar bending forces of approximately 90 nN were measured for a single forisome sequentially exposed to 10 mM Ca^{2+}, Sr^{2+} and Ba^{2+}. In the absence of dissolved oxygen, the same conditions resulted in averaged bending forces of (93 ± 40) nN, (58 ± 20) nN, and (91 ± 20) nN after contacting different forisomes with 10 mM Ca^{2+}, 10 mM Sr^{2+}, and 10 mM Ba^{2+} respectively, demonstrating that the force generated was independent on ion concentrations above a certain threshold value.

1. Introduction

Protein-based motors [1, 2] convert energy from chemical reactions directly into mechanical work. This is achieved through protein folding and unfolding, which is controlled by chemical reactions such as the protonation/deprotonation of amino and carboxylate groups, the formation of metal-protein complexes, and the phosphorylation/dephosphorylation of hydroxyl groups on serine and tyrosine residues. Some protein-based motors are dependent on nucleoside triphosphates [1], while others such as spasmonems [3 - 6] and forisomes [7 - 9] are propelled directly by Ca^{2+}. Spasmonems are isotropically-contracting aggregates of the protein spasmin, found in the stalks of *Vorticella* sp. Forisomes are aggregates of P-proteins, found in the phloem of legumes (*e.g. Vicia faba*) [10, 11]. In [10, 11] it was demonstrated that these protein aggregates rapidly disperse and occlude the pores of sieve plates between phloem cells after injury or by an osmotic shock induced under *in vivo* conditions. In the presence of free Ca^{2+}, Sr^{2+} or Ba^{2+}, longitudinally extended forisomes contract to a squatter, more swollen form [8, 12]. A thermodynamic cycle process [12] can be completed by the extraction of these ions with ethylene diaminetetraacetic acid (EDTA), during which the forisomes revert to the longitudinally extended state.

During such contractions, forisomes generate forces of approximately 100 nN [8, 13, 14] in comparison to spasmonems which generate 40–60 nN [15]. The threshold concentration of Ca^{2+} is between one and two orders of magnitude higher for forisomes [12] than for spasmonems [5]. However, taking into consideration earlier investigations [12 -14], there are at least two sources of energy for these contraction processes: the binding of Ca^{2+} ions to the functional groups of a large number of protein molecules and the con-

formational change of those protein molecules. Since only very small (<0.5%) volume changes occur during protein folding at normal pressure (even within tightly packed protein aggregates) [16, 17], and since forisomes increase in volume by up to 184% during contraction [12], the absorption of water needs to be considered as a potential source of energy. Energy could derive from tightly bound water molecules around hydrophobic side chains and polar groups as well as the relatively weak binding that occurs in hydrogels. Since forisomes swell significantly during contraction, volumetric work should also be considered. The predominant energy source and the behaviour of water molecules in the vicinity of the protein molecules of the forisomes remain to be determined.

Here we describe a comparative investigation of the influence of selected metal ions on the changing geometric parameters of contracting forisomes, the threshold values of the cooperatively conformational changes as well as the strength and dynamics of forces underlying forisome conformational changes induced by metal ions and pH shifts. The first time, the generated forces were measured as a function of the concentration of Ca^{2+}-, Sr^{2+}- and Ba^{2+} ions and in dependence on the pH value. Another aim of this work was to determine the apparent dissociation constants of Ca^{2+}, Sr^{2+}, and Ba^{2+} ions bound in the forisomes unloaded and loaded with a bending force.

2. Materials and methods

2.1. Isolation and purification of forisomes

Forisomes were isolated from *Vicia faba* plants as described elsewhere [8, 9, 12]. The plants were grown in pots of sterilized soil in a glasshouse for 6 weeks and then thor-

oughly irrigated. The first free internodes were excised and placed in the Ca^{2+}-free M - buffer containing 10 mM EDTA, 0.1 M KCl and 10 mM Tris (pH 7.3). The rind was peeled off the stalk in two strips, and the separated, pre-dried phloem tissue was powdered under liquid nitrogen and suspended in the same Ca^{2+}-free solution. The suspension was filtered through a 55-μm nylon mesh and the filter cake was rinsed several times with small amounts of the Ca^{2+} - free solution.

2.2. Measuring cell

The apparatus for measuring the force generated by individual forisomes (measuring cell) was set up as shown in **Figure 1**. The cell consisted of a measuring chamber (MC) with the inflow (I) for the reagent and conditioning solutions, the outflows (O1 and O2), a transfer channel (TC) and the storage chamber (SC). The flow and exchange of conditioning and rinsing solutions were adjusted by three computer-controlled piston pumps (Metrohm Dosimat 665, Herisau, Schwitzerland). Two or three pumps were combined to mix stock solutions, adjust the concentrations of bivalent metal ions and EDTA, and modulate the pH value.

The measuring cell was mounted on a thermostatic microscope table (Axiovert 25 C, Zeiss, Jena, Germany) adjusted to 298.3 ± 0.5 K. The microscope was automated as described by Francke [18]. Two micromanipulators (Luigs & Neumann) with automatic *xyz* adjustment were mounted on the opposite sides of the microscope table. The first micromanipulator (Mm1) held a glass pipette with a long pulled tip (diameter <2 μm) serving as the stator. The second micromanipulator (Mm2) held a bending glass fibre

(BF) 1.5–3 mm in length and with a diameter of 9 μm. With the exception of the pumps, the entire measuring cell was mounted on an actively dampened optical bench.

A video camera (JVC TK-C1481BEG, JVC, Japan) was installed on the microscope and connected to a PC by a frame grabber card (HaSoTec GmbH, Rostock, Germany). A home-made software package [18, 19] was developed for automatic control of the microscope, the piston pumps and the image processing. The video images and films were evaluated by correlation analysis of digital grey patterns with a shifting reference window [20,21] using ARAMIS Software (GOM mbH, Braunschweig, Germany) or the image processing program Analysis 3.1 (SIS Soft Imaging System GmbH, Münster, Germany).

For scanning electron microscopy (SEM), forisomes were purified from crude preparations by centrifugation in a Nycodenz® density gradient, freeze dried as described previously [8] and resuspended in Ca^{2+}- free medium. Some batches were incubated in 10 mM Ca^{2+}, 0.1 M Tris (pH 7.3) to study longitudinally contracted forisomes. Droplets of the suspension were transferred to custom-made patches of nanoporous Al_2O_3 membranes [22] or microporous polycarbonate membranes, and forisomes were allowed to settle. After primary fixation in buffered 2.5% glutaraldehyde in 4.3 mM Na_2HPO_4, 1.4 mM KH_2PO_4, 137 mM NaCl, 12.7 mM KCl adjusted to pH 7.5 with phosphate-buffered saline (PBS), the samples were washed three times with PBS for 5 min and post-fixed with 2% OsO_4 in PBS for 2 h. The OsO_4 solution was then replaced by distilled water. The loosely bound water was progressively removed by sequential immersion in water/acetone mixtures (75%, 50%, 30%, 10%, 5%, and 0%; 10 min each). After the final step, the samples were dried in a critical point dryer (CPD 030, Bal-Tec, Balzers, Liechtenstein) with liquid CO_2. The nanoporous alumina membrane patches were fixed on

holders and sputtered with platinum (up-graded sputter-coater B30, VEB Hochvakuum-technik, Dresden, Germany). They were inspected using a cold field emission SEM (S4500, Hitachi, Tokyo, Japan) at accelerating voltages of 1 to 10 kV.

2.3. Measurement of the force generated by forisomes and analysis of geometric parameters

Single forisomes were captured on a thin glass pipette tip in the storage chamber and drawn through the small transfer channel (TC, Figure 1) 5 mm in length and 1 mm wide into the measuring chamber under slight reverse flow of M - buffer (Figure 1). To measure geometric parameters, single *in situ* purified forisomes were fixed at the tip of the micropipette by self-adhesion on the glass surface. The forisomes were aligned by the flow of the conditioning solution before the flow was stopped and image processing commenced. The diameter (D_F) and length (L_F) of each forisome were determined by image processing (**Figure 2**). Approximate volumes (V) were calculated according to equation (1), given the assumption that forisomes from *Vicia faba* normally have a rotationally symmetrical ellipsoid shape.

$$V = 1/6\ \pi D_F^2 L_F, \qquad (1)$$

To measure the force generated by forisome contraction, the free end of the forisome was fixed to the tip of a bending glass fibre (Advanced Glassfiber Yarns LLC, Aiken,

SC, USA) with a diameter of 9.0 μm and a Young module of 87 $kNmm^{-2}$ [23]. The stiffness of the bending fibre was adjusted by its length L_b. The fibre diameter was measured by raster electron microscopy and the length by light microscopy. The Young module of 87 kN/mm² [23] was verified by both micro tensile and micro bending tests. Both the bending fibre and the forisome were completely immersed in the measuring solution to exclude any forces at the liquid/air phase interface. The angle between the long axes of the forisome and bending fibre was fixed at 88–92° by aligning the forisome in the flowing solution, which was orthogonal to the initial position of the bending fibre. The flow was stopped after alignment was achieved. Thereafter, the forces generated by the contracting forisome were measured using images of the bending fibre captured under the video microscope as demonstrated earlier [13] and correlation between the digital patterns of a predefined window of observation, before and after bending of the glass fibre (**Figure 3**).

The displacement of the fibre tip was calculated from the shifting vectors determined from the initial window and the shifted window with maximum correlation.

A thin glass fibre can be bent by a contracting forisome fixed on its ends between the tip of a stator and the glass fibre tip as shown earlier by Knoblauch *et al.* [8] and by our own investigations [12, 13]. Mechanical work is performed according to equation (2) given a linear displacement (Δx) of the fibre tip. The force can then be calculated according to equation (3) where E is the Young module, d is the diameter of the glass fibre, and L_b its length.

$$W_{mech} = ½ F \bullet \Delta x \quad (2)$$

$$F = \frac{3\pi E d^4}{64 L_b^3} \bullet \Delta x \quad (3)$$

2.4. Analysis of metal ion concentration and pH variation

The concentrations of the free divalent metal ions Ca^{2+}, Sr^{2+} and Ba^{2+} were adjusted by titration with EDTA or *vice versa* in a stirred vessel. Both the metal ion and the EDTA solutions were prepared in the buffer M containing 200 mM Tris, 0.1 M KCl and 10 mM of equilibrated D-glucose, adjusted to pH 7.3. The stock solutions of metal ions were mixed with a stock solution of EDTA in a magnetically stirred vessel to a final volume of 20 mL before force measurements were carried out.

The metal ion stock solutions were prepared by dissolving precisely weighed amounts of $Ca(NO_3)_2$, $Sr(NO_3)_2$ and $Ba(NO_3)_2$ in deionized and bi-distilled water. The exact metal ion concentrations were adjusted by diluting with the M – buffer. The free metal ion concentrations were calculated using known conditional equilibrium constants. The dissolved

oxygen was eliminated in a two-step enzymatic reaction comprising 2 – 3 U/ml glucose oxidase and 10 - 15 U/ml catalase (both from SIGMA, Taufkirchen, Germany) in the M-buffer solutions. The elimination of dissolved oxygen was based on reactions (4) and (5) and was fast enough to suppress back-diffusion of oxygen from the atmosphere.

$$\beta\text{-D-glucose} + O_2 \rightarrow \text{D-gluconate} + H^+ + H_2O_2 \quad (4)$$

$$2H_2O_2 \rightarrow O_2 + 2H_2O \quad (5)$$

The oxygen concentration was monitored in the inlet and outlet solutions of the measuring chamber using a Clark-type pO_2 sensor (Oxi3000, WTW GmbH, Weilheim, Germany). The oxygen concentration was lower than 3 μM and could be maintained below this value at the immersed forisome. The backdiffusion of oxygen from the surrounding air to the forisome under investigation is clearly overcompensated by the high rates of the enzyme-catalyzed reactions (4) and (5) for at least 12 h under continuous flow.

To implement pH induced conformational changes in forisomes the M-buffer is replaced either by 200 mM sodium acetate/acetic acid/ 0,1 M KCl buffer adjusted to pH 4.5 or by 100 mM glycine/100 mM NaCl buffer adjusted to pH 11.0.

3. Results and Discussion

3.1 Influence of different metal ions on the geometric parameters of forisomes

Forisomes change from a longitudinally expanded form to a contracted and swollen form in the presence of divalent metal ions Ca^{2+}, Sr^{2+}, and Ba^{2+} [12–14]. To gain a deeper insight into the molecular mechanisms involved in this process, we investigated the binding strength of metal ions with different radii in the absence of dissolved oxygen. The enzymatic elimination of dissolved oxygen was rapid and reliable, excluding the potential impact of oxidative deactivation. By sequentially contacting forisomes with concentrations of Ca^{2+}, Sr^{2+}, and Ba^{2+} changing from zero to 10 mM in M-buffer interrupted by rinsing with 10 mM EDTA in the same buffer, the same forisomes showed in these experiments almost the same changes of both their normalized diameter D_F /$D_{F,o}$ and normalized length L_F/$L_{F,o}$ as demonstrated in **Figure 4**. $L_{F,o}$ and $D_{F,o}$ are the initial length and the initial diameter of the forisome, respectively. L_F and D_F are the time-dependent measuring values. Pairs of experiments were carried out each on the same forisome and repeated four to five times to compare the changes of its length induced by Ca^{2+} and Sr^{2+}, Ca^{2+} and Ba^{2+}, and Sr^{2+} and Ba^{2+}. The differences between the changes of the L_F/$L_{F,o}$ values were smaller than 5 % if measured at the same forisome.. Both experiments were carried out three times (results not shown). The exact time-dependent concentrations changing continuously from approximately zero to 10 mM of metal ions could be calculated from the hydrodynamic mixing model in the measuring cell taking into consideration the fast reaction between EDTA and the metal ions. The investigated divalent ions had very similar effects on the normalized length and diameter of the corresponding forisomes.

Approximately the same amount of water is taken up and the forisome assumes the same ordered structure (**Figure 5**) suggesting the water is bound tightly to the forisome proteins regardless of the divalent ion present in solution.

Therefore, in the absence of dissolved oxygen, any changes in geometric parameters and the uptake of water seems to be independent of the ion radius and the strength of binding between the metal ions and the protein molecules responsible for forisome conformational transformation. An increase in KCl concentration from 0.5 mM to 4.0 M had no significant influence on the geometric shape of the longitudinally expanded forisomes supporting the conclusion that neither osmotic effects nor the increase of ionic strength alone can induce contraction (results not shown).

For the first time the conformational transition of forisomes was investigated with respect to cooperativity n and strength of chemical binding of Ca^{2+}, Sr^{2+} and Ba^{2+} ions, expressed as apparent dissociation constants $K_{m.}$ Almost the same amount of water is taken up and the forisome assumes the same ordered structure (**Figure 5**) suggesting the water is bound tightly to the forisome proteins regardless of the divalent ion present in solution. **Figure 6** shows the averaged titration curves for forisomes exposed to Ca^{2+}, Sr^{2+} and Ba^{2+}, at first time performed for Sr^{2+} and Ba^{2+} ions to get a more detailed comparison. Using Hill plots based on equation (6), we calculated the apparent binding constants and apparent number of divalent ion-binding sites in the contracting protein molecules. The results are summarized in **Table 1**, where L_F^* is defined by equation (7), where $L_{F,min}$ and $L_{F,max}$ represent forisome length in the completely contracted and expanded states, respectively.

$$\lg((1-L_F^*)/L_F^*) = n \bullet \lg[Ca^{2+}] - n\lg K_m$$

(6)

$$L_L^* = (L_F - L_{F,min})/(L_{F,max} - L_{F,min})$$

(7)

The binding strength, expressed by the apparent dissociation constants K_m, between the divalent metal ions and the forisome proteins appears to decrease with increasing radius of the metal ions, resulting in larger dissociation constants. Therefore, the inflection points and threshold values of the ion concentrations during forisome contraction are much higher for Sr^{2+} and Ba^{2+} compared to Ca^{2+}. The binding of Sr^{2+} and Ba^{2+} also showed a higher degree of cooperativity, as shown by their higher averaged n-values 5.0 and 6.0, respectively, in comparison to the approximate and averaged value n = 2 measured for Ca^{2+}-ions. Since we studied different forisomes, the different degrees of contraction (**Figure 6**) did not contradict the independence of contraction on the chosen metal ion as had been assumed before.

3.2. Force generation during switching by selected bivalent metal ions

The forisomes were fixed between the tips of a stiff glass pipette and a flexible glass fibre. It should be noted that the forisomes become spontaneously fixed to the glass through chemisorption between unmodified glass and at least the outer protein shell of the forisome, allowing it to withstand forces of at least 300 nN without detachment. In the contracted, swollen state the binding force between the forisome and the glass surface is considerably higher than in the longitudinally stretched state where they can be detached relatively easy from the glass surface. However, after only one con-

traction and stretching cycle, the forisomes remain strongly chemisorbed on the glass tips. **Figure 7** shows the time-dependence of the lengths of the stretched and contracted forms of three different forisomes. These forisomes contracted in the presence of 50 μM Ca^{2+}, 150 μM Sr^{2+} and 2 mM Ba^{2+}, respectively, and remained in this loaded state for the next 30 minutes. The ratio of the lengths $R = L_{Fc}/L_{Fc,o}$ of the contracted forisomes decreased over the entire 30 min by only 0.09–0.92% in the stretched state. $L_{Fc,o}$ is the final length of the contracted forisomes immediately measured after the end of its contraction. L_{Fc} is the length of the corresponding forisome measured thereafter in dependence on time. The averaged loads were 93 nN for Ca^{2+}, 37 nN for Sr^{2+}, and 81.5 nN for Ba^{2+} for eight different forisomes. Therefore, the forisomes were able to keep their shape stable in the contracted state. The relatively high stability of forisome length in the contracted state under load reveals the surprisingly high mechanical stability of the forisome protein scaffold.

Our preliminary results [13] are extended here into a detailed investigation of the physicochemical behaviour of the forisomes under load in comparison to the measuring results obtained in the absence of load. For the first time the force generation by Ca^{2+}-, Sr^{2+}- and Ba^{2+}-ions were investigated during step wisely performed titration experiments in the absence of dissolved oxygen taking into consideration the different binding strengths of these ions and the cooperativity of its binding. The conformational transition of forisomes was observed as a function of defined metal ions concentrations comparing the behaviour under load and in the absence of load.

However, the load should have a significant influence on the geometric parameters of the forisomes in their final states. We therefore titrated several forisomes with Ca^{2+},

Sr^{2+} and Ba^{2+}, initially in the absence and then in the presence of the bending load. **Figure 8** compares the corresponding changes in normalized forisome lengths according to the metal ion concentration. Under load the change of length and diameter of the forisomes is strongly decreased. Assuming the same free reaction energy one can assume that under load a smaller part is converted into the volumetric work $p\Delta V$ with the pressure p and the change of the forisome volume.

The forces generated during this experiment cause the amplitudes of the lengths to decrease by 15% (Ca^{2+}), 11% (Sr^{2+}) and 9% (Ba^{2+}), for the complete conversion of the fully extended forisome to the fully contracted state. The final and averaged bending forces of 93 nN for Ca^{2+}, 58 nN for Sr^{2+} and 91 nN for Ba^{2+} were in the same order of magnitude and demonstrating the apparent independence of the selected metal ion. Earlier published measurements [13] support this conclusion. In that experiment the same forisome was successively contracted with 10 mM Ca^{2+}, 10 mM Sr^{2+} and 10 mM Ba^{2+}, each replacement being preceded by a 10-min rinse with 10 mM EDTA in M-buffer. The same stationary force of approximately 90 nN was determined for all three metal ions.

Table 2 summarizes the parameters n and K_m calculated from the Hill model as well as the normalized changes f_V of the forisome volume each time for five different forisomes investigated for one kind of metal ion. f_V is defined according to equation (8), where $V_{contracted}$ is the measured volume of the contracted forisome and $V_{expanded}$ is the initial volume of the longitudinally expanded forisome.

$$f_V = \frac{V_{contracted} - V_{expanded}}{V_{contracted}} \qquad (8)$$

Under the load caused by fibre bending the mean apparent dissociation constant K_m increased in comparison to those determined without load. With respect to K_m, the outer force shifts the equilibrium to a slightly enhanced dissociation according to equation (9), where $\triangle_B G$ is the free reaction energy of binding. Under load, the normalized change of forisome volume decreased. The change of the cooperativety n is not significant. However, with increasing dissociation constants, the minimum of metal ion concentrations must also be increased to initiate the change of forisome conformation from the longitudinally expanded to the contracted and swollen state.

According to equation (9), an outer stretching force F will shift the equilibrium in the direction of forisome proteins with a lower content of metal ions, and Ca^{2+}, Sr^{2+} or Ba^{2+} will be released. This process is combined with the release of water according to the well known and broadly investigated behaviour of the forisomes during longitudinal expansion. Further investigations at different temperatures, and of the Ca^{2+}, Sr^{2+} and Ba^{2+} release as a function of load, will be necessary to separate and quantify these effects.

$$\triangle_B G + ½ F \cdot \triangle x = RT\ln K_m \qquad (9)$$

The relative independence of geometric parameters D_F and L_F, and the generated

forces on the type of metal ion hints that the folding of proteins is the source of the generated mechanical force. It is widely known that protein folding always involves the binding and release of water molecules. It can be assumed that a significant proportion of the absorbed water is bound to hydrophobic amino acids [24]. The strong forces generated (43 - 120 nN) and the relatively high energy densities estimated by comparing the bending work to the initial forisome volumes (230-800 Jm^{-3}) support this hypothesis.

3.3 Force development induced by pH shifts

For the first time, the force generation was measured during the earlier demonstrated [8,12] conformational transition of forisomes initiated by pH changes. To achieve a better understanding of the conformational transition of the forisomes and their mechanism the force generation induced by pH changes both in the acid and in the alkaline range was compared to that induced by twofold charged metal ions.

Because the alternative divalent metal ions generate approximately the same force in a single forisome and very similar forces in different forisomes, we investigated the geometric contraction behaviour of additional forisomes and the forces generated in two pH ranges: 4.5–7.3 and 7.3–11. In the absence of any load, the mean normalized volume increased by a factor f_V of 1.9 ± 0.6 for changing from pH 7.3 to 4.5 and increased by a factor of 3.9 ± 1.1 for changing from pH 7.3 to 11.0 as shown earlier [12]. These averaged values were determined by measuring 13 different forisomes and show very different swelling behaviours in the alkaline and acid ranges. **Figure 9** shows how the force generated by the forisomes changes as the pH is reduced from 7.3 to 4.5, and as it is increased from 7.3 to 11.0. Both experiments on two dif-

ferent forisomes produced similar final forces of approximately 120 nN. However, very different volume-specific forces of 1.21 μN/nL and 0.52 μN/nL were measured during the changes from pH 7.3 to 4.5 and from pH 7.3 to 11.0, respectively. The different response kinetics could be explained by the very different volumes of 188 fL and 900 fL estimated for the longitudinally expanded forisomes.

The normalized volumes changed by factors of 1.29 and 1.75 during the changes from pH 7.3 to 4.5 and from pH 7.3 to 11.0, respectively. It follows that in both experiments, the swelling was significantly lower than in the load free state. As we found for forisome contraction induced by divalent metal ions, loading reduces the amount of absorbed water. These pH changes generate similar mechanical forces in comparison to the conformational transition induced by the bivalent metal ions. Since the metal ion and the pH induced conformational changes also show similar changes in relative volume and water uptake, the molecular mechanisms are likely to work in analogous ways. We propose that the swelling of a protein aggregate with a very high tensile stability, initiated by an unfolding event, is the common principle. The ions Ca^{2+}, Sr^{2+}, and Ba^{2+} as well as protons and hydroxide ions at pH < 4.9 and pH > 10.8, respectively, initiate the folding of at least a part of the protein molecules in the forisomes. It is assumed that according to Knoblauch and Peters [7] repelling electrical charges localized in protein molecules are compensated inducing their conformational change. Based on the very similar bending forces independently of the kind of induction by metal ions and pH changes it can further be assumed that the amplified uptake and especially the binding of water is the thermodynamic driving force of contraction and swelling of the forisome essentially determining the changes

of both the geometrical parameters and the force generation of the forisome. The high mechanical stability of the forisome shape under load combined with a significant degree of swelling support the assumption of tightly binding of water. We propose that the swelling of the protein aggregate – forisome - with a very high tensile stability, initiated by an unfolding event, is the common principle of the conformational change of the forisome.

4. Conclusions

Since at least the metal ion-induced conformational change in forisomes is fully reversible in the absence of dissolved oxygen, we conclude that the binding and release of selected divalent metal ions, or simply a pH shift, can induce a highly cooperative folding process in the forisome followed by the uptake and strong binding of water molecules. Two groups of water molecules can be distinguished: strongly bound molecules that cannot be released by an outer tensile force of up to at least 120 nN, and weakly bound molecules released by smaller tensile forces. Cooperative protein folding into a similar conformational state combined with the corresponding binding of additional water molecules seems to be the force underlying this process, as supported by the almost complete independence of load-free forisome conformational change on the type of metal ions present. The hypothesis is further supported by the very similar stationary forces measured on many forisomes induced both by three different metal ions and pH shifts into the alkaline and acid pH ranges.

Acknowledgements

The authors would like to thank A. Cismak for the SEM images of the forisomes and M. Knoblauch, W. Peters, D. Prüfer and G. Noll for helpful discussions. The work was supported by a Fraunhofer Gesellschaft internal research program.

References

[1] J. Howard, Mechanics of motor proteins and Cytoskeleton. Sinauer Associates Inc., Sunderland, MA, (2001).

[2] R.D. Vale, Millennial musings on molecular motors, Trends in Cell. Biol. 9 (1999) 493 – 505.

[3] H. Hoffmann-Berling, Der Mechanismus eines neuen, von der Muskelkontraktion verschiedenen Kontraktionszyklus, Biochim. Biophys. Acta 27 (1958) 247 – 255.

[4] W.B. Amos, Reversible mechanochemical cycle in the contraction of *vorticella*, Nature 229 (1971)127 – 128.

[5] H. Asai, T. Ochiai, K. Fukui, M. Watanabe, F. Kano, Improved preparation and cooperative calcium contraction of glycerinated vorticella, J. Biochem. 83 (1978) 795 – 798.

[6] Y. Moriyama, H. Okamoto, H. Asai, Rubber – like elasticity and volume changes in the isolated spasmoneme of giant zoothamnium sp. under Ca^{2+} - induced contraction, Biophysical. J. 76 (1999) 993 – 1000.

[7] M. Knoblauch, W.S. Peters, Forisomes, a novel type of Ca^{2+} - dependent contractile motor, Cell Mot Cytoskeleton

58 (2004)137 – 142.

[8] M. Knoblauch, G.A. Noll, T. Müller, D. Prüfer, I. Schneider-Hüther, D. Scharner, A.J.E. van Bel, W.S. Peters, ATP-independent contractile proteins from plants, Nature materials 2 (2003) 600 - 603.

[9] M. Knoblauch, G.A. Noll, T. Müller, D.Prüfer, I. Schneider-Hüther, D. Scharner D, A.J.E. van Bel, W.S. van Bel, *Erratum:* ATP-independent contractile proteins from plants (Nature Materials 2 (2003) 600 – 604.), Nat. Mater., 4 (2005) 353.

[10] M. Knoblauch and W.S. Peters, Reversible calcium-regulated stopcocks in legume sieve tubes, The Plant Cell 13 (2004) 1221 – 1230.

[11] K. Ehlers, M. Knoblauch and A.J.E. Van Bel, Ultrastructural features of well-preserved and injured sieve elements: minute clamps keep the phloem transport conduits free for mass flow, Protoplasma 214 (2000) 80 – 92.

[12] S. Schwan, M. Fritzsche, A. Cismak, A. Heilmann, U. Spohn, *In vitro* investigation of the contraction behaviour of chemomechanical P-protein aggregates (forisomes), Biophys. Chem. 125 (2007) 444 – 452.

[13] S. Schwan, M. Fritzsche, A. Cismak, G. Noll, D. Prüfer, U. Spohn, A. Heilmann, Micromechanical measurements on chemo-mechanical protein aggregates. Materials Research Society USA, Proceedings of the Fall Meeting, Boston, 27. – 30.11. 2006, 09750-DD-03-10.

[14] M. Fritzsche, Master Thesis, University of Halle – Wittenberg, (2005)

[15] Y. Moriyama, S. Hiyama, H. Asai, High-speed video cinematographic demonstration of stalk and zooid contraction of *Vorticella convallaria*, Biophysical J. 74 (1998) 487 – 491.

[16] Y. Harpaz, M. Gerstein, C. Chothia, Volume changes on protein folding. Structure 2(1994) 641 – 649.

[17] S. Abbruzzetti, E. Crema, L. Masino, A. Vecli, C. Viappiani, J.R. Small, L.J. Libertini, E.W. Small, Fast events in protein folding: Structural volume changes accompanying the early events in the N→I transition of apomyoglobin induced by ultrafast pH jump, Biophysical J. 78 (2000) 405 – 415.

[18] Ch. Francke, Diploma Thesis, University of Applied Sciences, Merseburg, 2004.

[19] S. Kneist, Diploma Thesis, University of Applied Sciences, Merseburg, 2006.

[20] Gelles J, Schnapp, BJ, Sheetz MP. Tracking kinesis-driven

movements with nanometre-scale precision, Nature 331 (1988) 450 – 453.

[21] Jähne, B. Digitale Bildverarbeitung, Springer, Berlin; Heidelberg; New York, 2002.

[22] A. Heilmann, N. Teuscher, A. Kiesow, D. Janasek and U. Spohn, Nanoporous aluminum oxide as a novel support material for Enzyme biosensors, J. Nanosci. Nanotechnol. 3 (2003) 1-5.

[23] 463 S-2 Glass Roving, Data sheet of Advanced Glassfiber Yarns LLC, Aiken, SC, USA 29801.

[24] W. Urry, Molecular machines: How motion and other functions of living organisms can result from reversible chemical changes, Angew. Chem. Int. Ed. Engl. 32 (1993) 819 – 841.

Figures and legends:

Figure 1 Design of the measuring cell. MC, measuring chamber; SC, storage chamber; TC, transfer channel; Mm1 and Mm2, micromanipulators; I, inflow; O1 and O2, outflows; BF, bending glass fibre; ST, stator tip; F Forisome.

Figure 2 Geometric parameters for the longitudinally expanded and contracted forms *V. faba* forisomes, $D_{F,c}$ and $D_{F,e}$ diameter of contracted and expanded forisome, respectively, $L_{F,c}$ and $L_{F,e}$ length of contracted and expanded forisme

Figure 3 Measuring the fibre bending by correlation of the digital image window before and after shifting.

Figure 4. Time dependencies of normalized forisome length $L_F/L_{F,o}$ (a) and diameter $D_F/D_{F,o}$ (b) after changing from the M-buffer to a M-buffer containing —△— 10 mM Ba^{2+}, —●— 10 mM Sr^{2+}, —□— 10 mM Ca^{2+} at pH 7.3 and T = 25°C.

Figure 5 A forisome imaged by FE-REM, 6 kV.

Figure 6 Comparison of titration courses of different forisomes immersed in M-buffer containing —△— Ba^{2+}, —●— Sr^{2+}, —□— Ca^{2+} with concentrations adjusted precisely

and stepwise form 0 to 10 mM, pH = 7.3**.**

Figure 7 Dependence of averaged (n = 4, measurements of four different forisomes for each metal ion) and normalized length $L_{Fc}/L_{Fc,o}$ of contracted forisomes on time in the presence of —●— 150 μM Sr^{2+}, —□— 50 μM Ca^{2+}, and —△— 2 mM Ba^{2+} dissolved in M-buffer at pH 7.3.

Figure 8 Forisome contraction induced by step wisely adjusted concentrations of (a) Ca^{2+} at bending loads (—●—) of F = 78 nN, of (b) Sr^{2+} at F = 43 nN, and of (c) Ba^{2+} at F = 92 nN compared to experiments performed at the same forisome for the corresponding ions and in the absence of load —○—, in M - buffer at 25°C and pH 7.3.

Figure 9 Time courses of force generation on two different forisomes, measured during the exchanges of M - buffer (pH 7.3) by the 50 mM sodium acetate/acetic acid buffer adjusted to pH 4.5 (—●—) and by the 50 mM glycine buffer adjusted to pH 11.0 (—○—), respectively.

Table 1 Titration of unloaded forisomes with Ca^{2+}, Sr^{2+}, and Ba^{2+}, measuring conditions as described in legend to Figure 5; ν = number of repeated measurements performed at different forisomes.

Divalent metal ion	Inflection point [μM]	Apparent dissociation constant K_D [μM]	Cooperativity n
Ca^{2+} (ν = 2)	25 ± 3	14 ± 2	2.0
Sr^{2+} (ν = 4)	75 ± 7	62 ± 7	5.0
Ba^{2+} (ν = 6)	1100 ± 11	1070 ±10	6.0

Table 2 Force titrations of forisomes with Ca^{2+}, Sr^{2+}, and Ba^{2+}, Measuring conditions as described in legend to Figure 9; ν number of repeated experiments performed at different forisomes in the absence of dissolved oxygen.

	normalized change of forisome volume		Average final force [nN]	Cooperativity n		Apparent dissociation constant K_m/μM	
	Under load	Without load		Under load	Without load	Under load	Without load
Ca^{2+}(ν=2)	4,9	5,8	93 ± 40	3.8	3.5	20.2	14,8
Sr^{2+} (ν=4)	2,5	3,2	58 ± 20	4.2	4.1	57.1	56,5
Ba^{2+}(ν=6)	5,6	6,8	91 ± 20	3.3	2.8	857	622

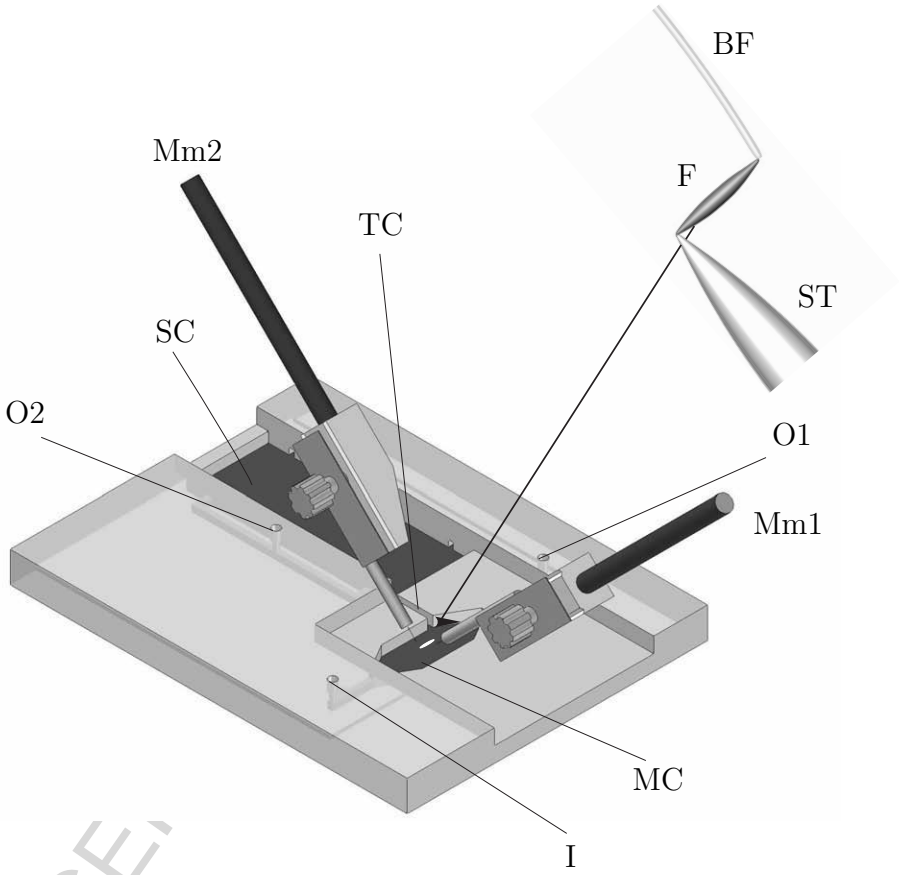

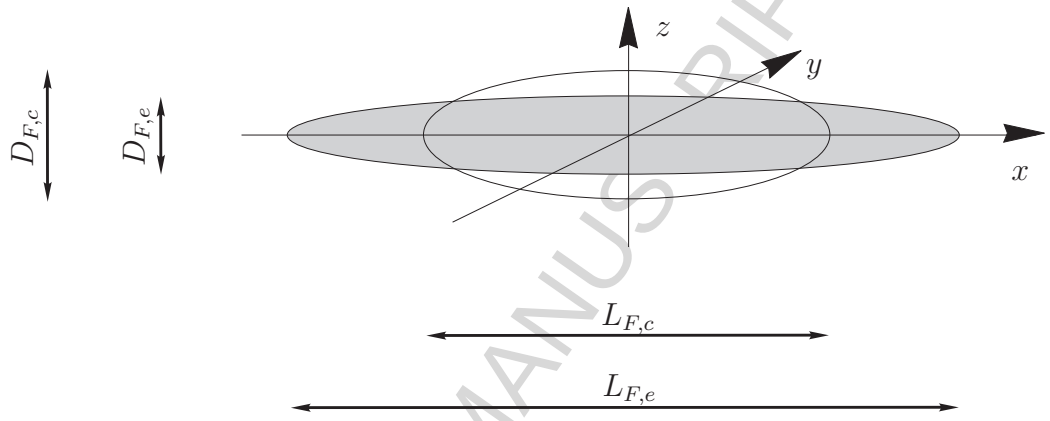

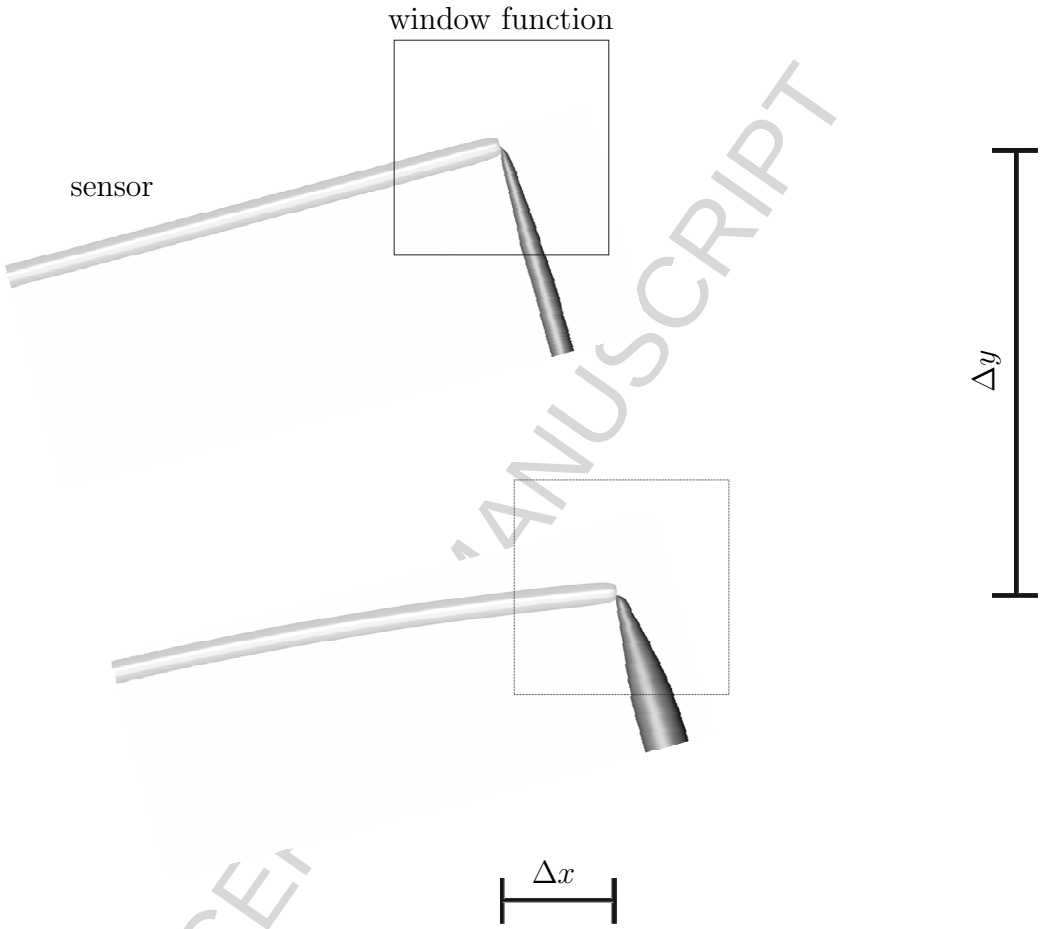

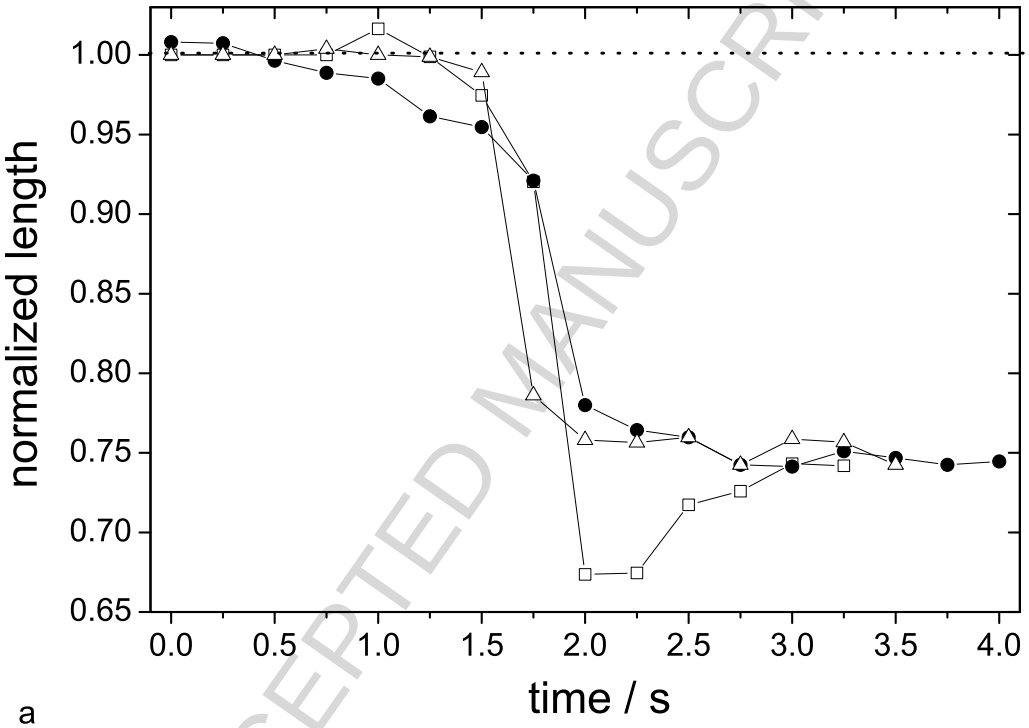

a

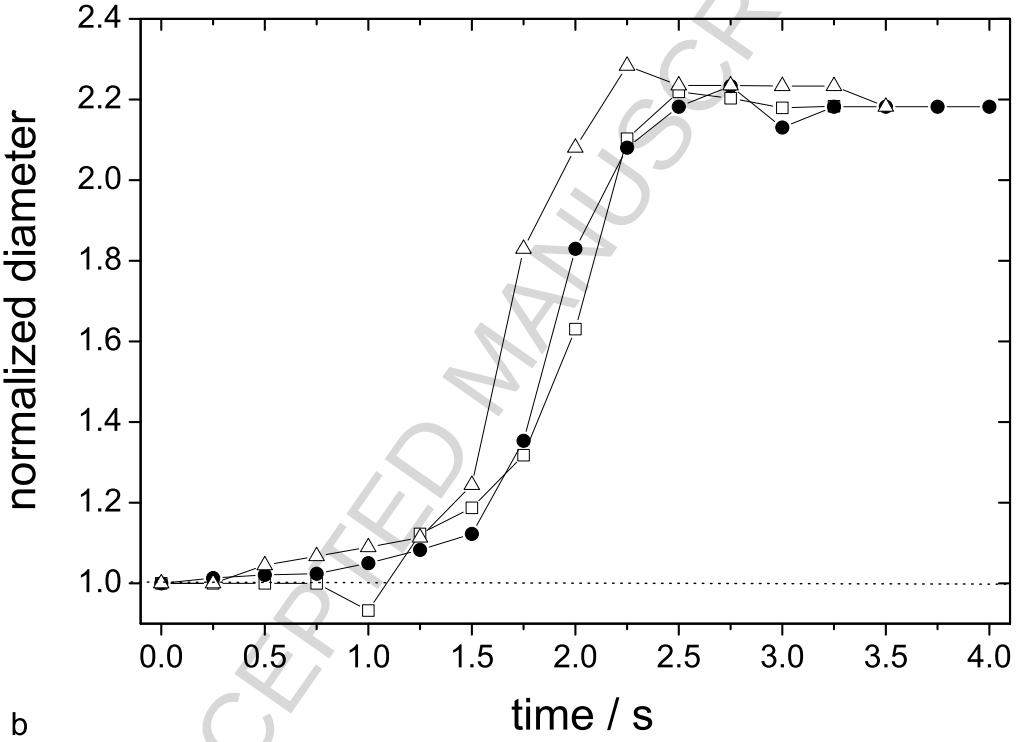

b

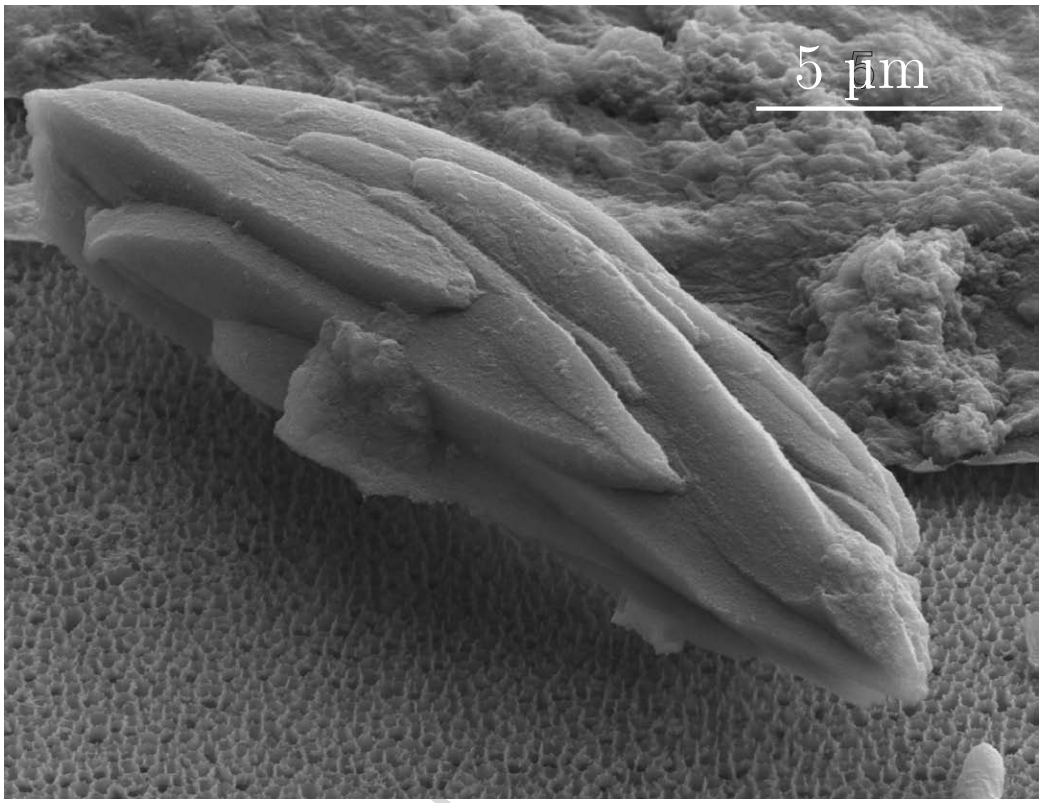

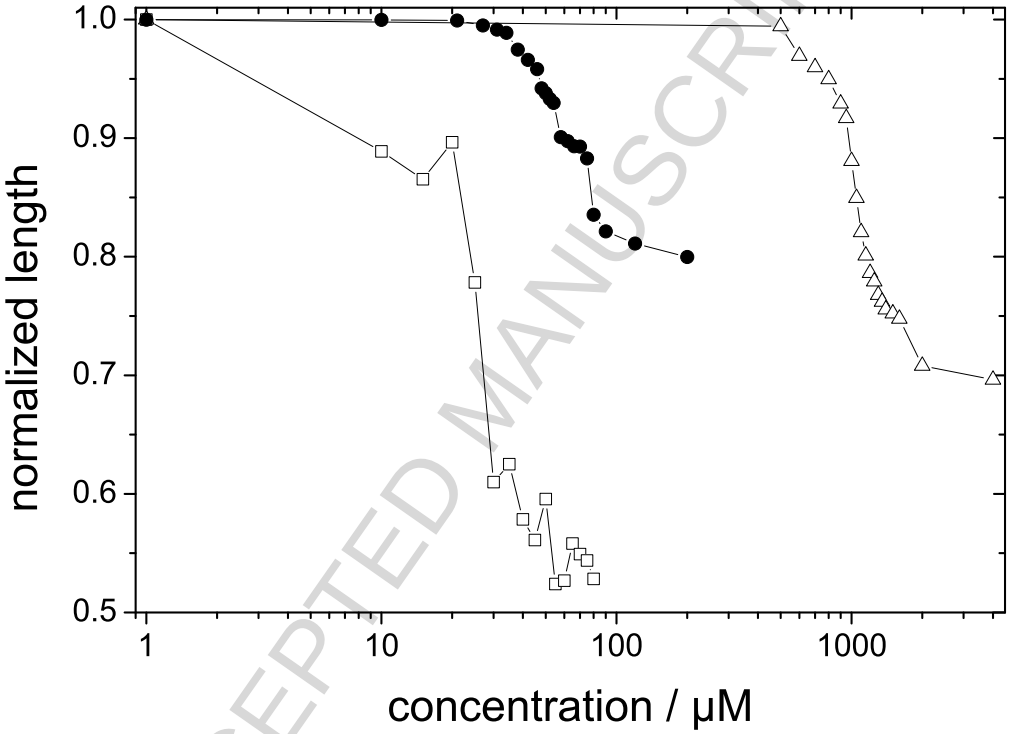

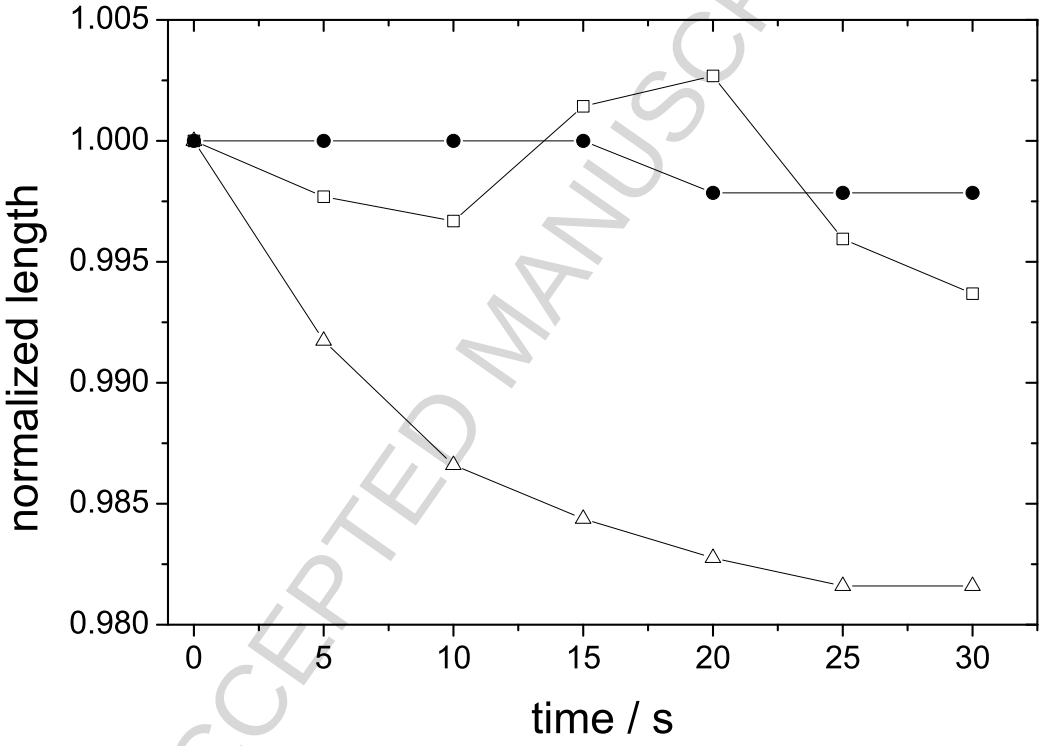

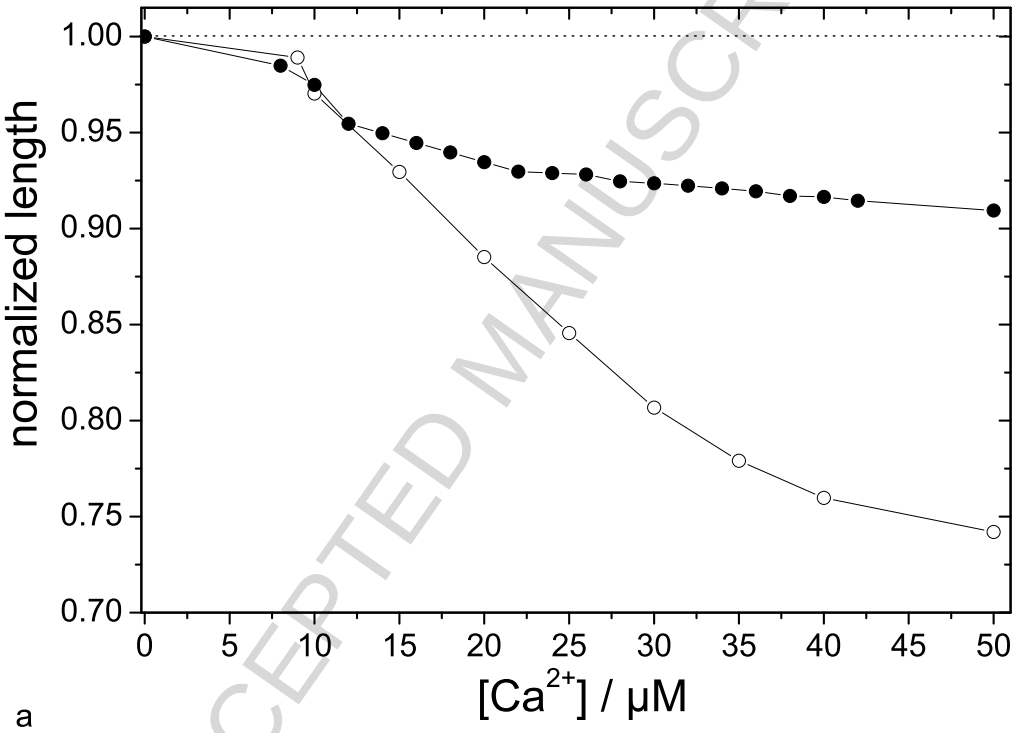

a

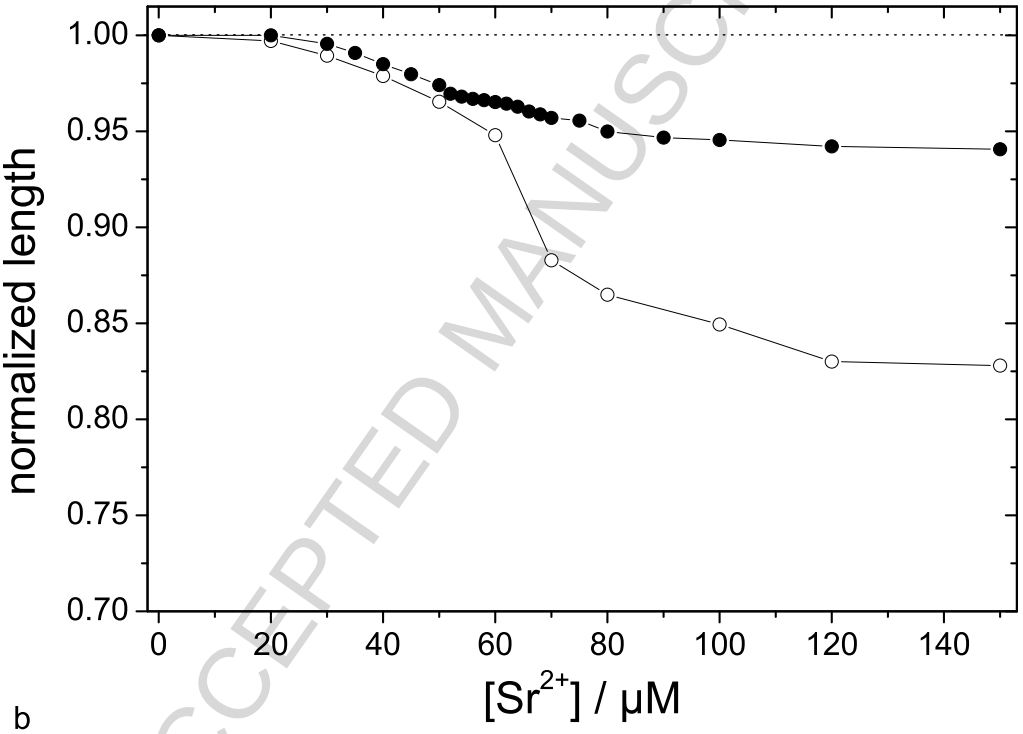

b

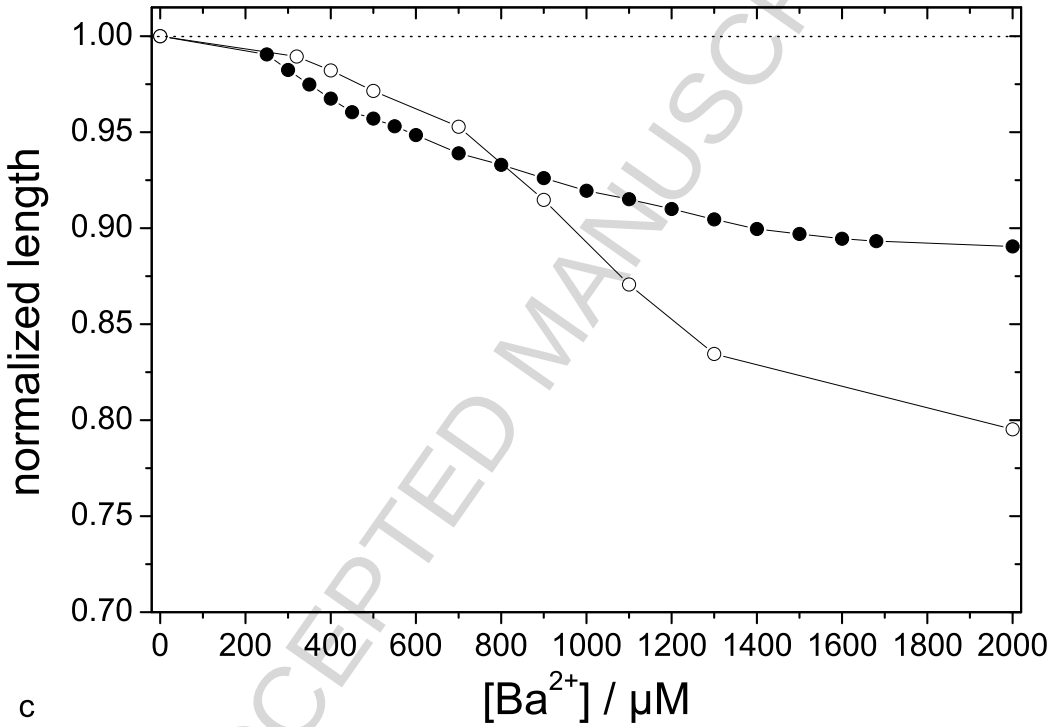

c